Thin Solid Films 518 (2010) 7283–7286

Contents lists available at ScienceDirect

Thin Solid Films

journal homepage: www.elsevier.com/locate/tsf

Size-dependent field-emission characteristics of ZnO nanowires grown by porous anodic aluminum oxide templates assistance

Chun-Hung Lai [a,*], Chia-Wei Chang [b], Tseung-Yuen Tseng [c]

[a] Department of Electronic Engineering, National United University, Miaoli 360, Taiwan
[b] Etron Technology, Inc., No. 6, Technology Road 5, Hsinchu Science Park, Hsinchu 30078, Taiwan
[c] Department of Electronics Engineering, National Chiao Tung University, Hsinchu 300, Taiwan

ARTICLE INFO

Available online 6 May 2010

Keywords:
Field-emission
Hydrothermal
Template
Field enhancement factor

ABSTRACT

The field-emission electrical properties of hydrothermally synthesized zinc-oxide nanowires grown on SiO_2–Si substrate are reported. Vertically aligned single-crystalline emitters with distinct length L and diameter D are realized by controlling the assisted growth of porous anodic aluminum oxide (AAO) templates. Field-emission measurement revealed that these field emitters exhibited controllable turn-on field E_{to} and the field enhancement factor β. Sample with feature size of $L=500$ nm and $D=80$ nm was prepared and then used as a basis for examining the size effect. Lower E_{to} and higher β were observed consistently for increasing the aspect ratio L/D. The enhanced properties of $E_{to}=1.48$ V/μm and β up to 6100 are achieved for $L/D=53$ ($L=1600$ nm and $D=30$ nm). Optimal characterizing parameters of E_{to} and β will be reached while pursuing extreme L/D practically. Factors such as the geometric limit of AAO template manufacture and the filling efficiency of ZnO into AAO pores will exert influence on the size-dependent effect.

1. Introduction

Zinc oxide nanowires (NWs) are promising semiconductor materials for applications in photonic and electronic devices, such as dye-sensitized solar cells [1], varistors [2], photodiodes [3], nanolasers [4], and gas sensors [5]. In addition, ZnO NW array has been proved to be a viable alternative as a field emitter due to its peculiar properties of oxide resistibility and high chemical stability, as compared to carbon nanotubes (CNTs). For emitter application, the turn-on field E_{to} and the field enhancement factor β are two dominant parameters characterizing the emission efficiency. Some effective methods, such as plasma bombardment [6], thermal annealing, or metal element doped [7], are adopted desirably to achieve highest current density at lower onset voltage [8]. Topics in focus are on examining the morphological variations based on various ZnO nanostructures [9–13], geometrical factors like the areal density of NWs and the distance between emitters and anode are also investigated [14,15]. However, studies on the influence of the emitter's aspect ratio are rare due to the difficulty in growth controllability, especially for ZnO NWs.

Growth of ZnO nanostructures can be obtained by vapor–liquid–solid method (VLS) [16], metal–organic chemical vapor deposition (MOCVD) [17], and thermal evaporation [18]. In this paper, we demonstrated the hydrothermal process in aqueous solution at temperatures below 100 °C [19], and then grew the NWs by porous anodic aluminum oxide (AAO) template without use of seeding layer or catalyst [20]. These emitters size was controlled by the template anodizing conditions to help observe directly the size effect, i.e., the corresponding E_{to} and β for different L and D.

2. Experimental details

The AAO template was prepared on a p-type SiO_2–Si (100) substrate. Pure Al film was deposited by thermal evaporation and then annealed at 400 °C for 5 h in Ar atmosphere. A two-step anodization process followed by the pore widening treatment was adopted to produce straight and uniform nanopores with desired diameter, density and length. The anodization was performed in a 0.3 M oxalic acid at 12 °C with an anodizing voltage of 50 V for 20 min. The as-prepared AAO film was wet chemically etched with a mixture of phosphoric acid and chromic acid at 60 °C. AAO surface at this stage exhibited a relatively ordered indent pattern. Using same anodizing voltage in the next step to give consistent interpore distance [21], the sample was further anodized under similar conditions. The resulting AAO nanochannel with length of 1 μm approximately was observed after reaction time of 6 min. Finally, after ultrasonic cleaning in de-ionized water and then by dipping in 5% phosphoric acid solution, the pore diameter was widened to be 80 nm for about 40 min. The synthesis of crystalline ZnO–NW was completed by putting into an aqueous solution (Milli Q, 18.2 MΩ-cm) of zinc nitrate hexahydrate ($Zn(NO_3)_2$–$6H_2O$, 0.01 M) and diethylenetriamine (HMTA, $C_6H_{12}N_4$, 0.01 M) in a sealed vessel at 95 °C for 1–2.5 h [19]. Overflowing top-covered ZnO was removed in HNO_3 solution and the final NW size L

* Corresponding author.
E-mail address: brandon@nuu.edu.tw (C.-H. Lai).

0040-6090/$ – see front matter © 2010 Elsevier B.V. All rights reserved.
doi:10.1016/j.tsf.2010.04.091

and D was determined by SEM images. The field-emission (FE) characteristics were conducted by a Keithley 237 current–voltage analyzer in a vacuum chamber at a base pressure of 5×10^{-6} Torr at room temperature. A copper electrode probe of area $A=0.00709$ cm^2 was placed at a distance around $d=200$ μm from the tips of the NWs. The test scheme is illustrated in Fig. 1. We use A and d for transforming current–voltage (I–V) data to current density and electric field (J–E), in which we assume $(d+L)\approx d$ for now $L\ll d$.

3. Results and discussion

3.1. Template and nanowire growth

Fig. 2(a) shows the typical SEM micrograph of AAO template. Deliberate growth of controlled template size (channel length L and pore diameter D) is the key in present work. Synthesized by low-temperature hydrothermal procedure at 95 °C via these vertically assisted AAO templates, the as-prepared ZnO NWs in this study show main diffraction peak (002) of wurtzite structure by XRD patterns. Fig. 2(b) shows the TEM cross-section image of AAO full of ZnO. Studies are conducted based on the same crystal structure and emitter's number density. The controlled NW size of varied L and D is obtained by different treatment duration of stable porous growth and different widening time for AAO template. Although the size of pore length and diameter is nearly proportional to the reaction time under the same electrolyte kind, concentration and temperature, the actual size after the ZnO NW formation and etching is acquired from SEM images.

3.2. E_{to}–β interdependence

Fig. 3 shows the FE characteristics for ZnO NW size of $L=500$ nm and $D=80$ nm. One can get E_{to} of 4.9 V/μm at current density of 1 μA/cm^2. As for the extraction of β, the Fowler–Norheim plot, $\ln(J/E^2)$ versus E^{-1}, is depicted in the inset. The linearity indicates the F–N relationship fits well the measured data. The F–N equation is as follows:

$$J=\frac{A\beta^2E^2}{\phi}\exp\left(\frac{-B\phi^{3/2}}{\beta E}\right)$$

where J is the current density, E the applied field, ϕ the work function of ZnO (5.37 eV), β the field enhancement factor, $A=1.56\times10^{-10}$

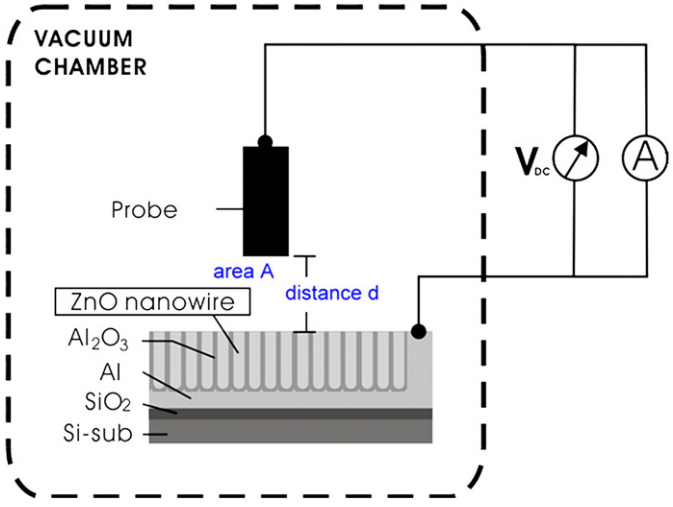

Fig. 1. Schematic test system for FE measurements, in which the probe-tip distance d is much larger than the NWs length L.

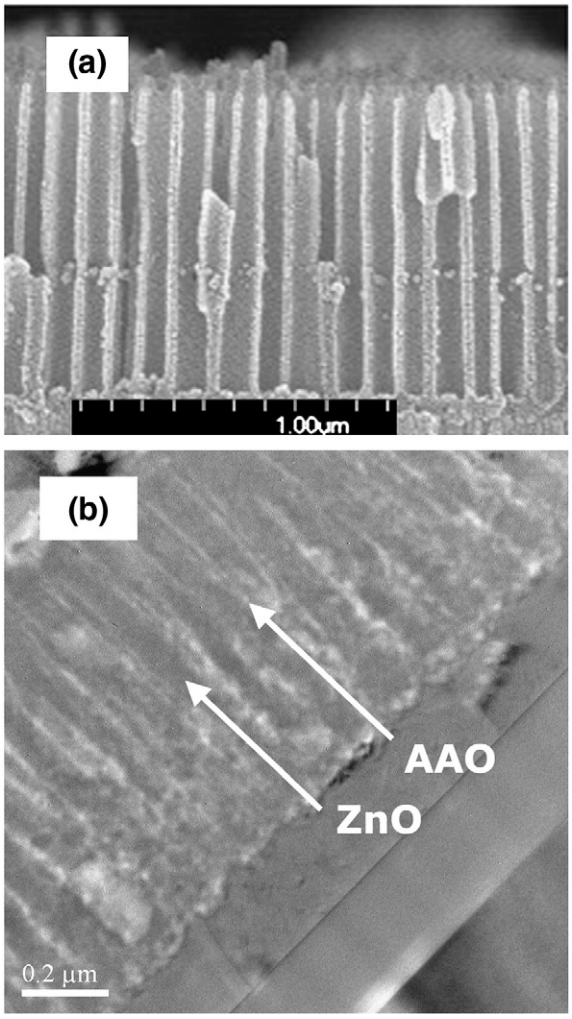

Fig. 2. (a) The typical SEM cross-section images of the AAO template used as an aid to prepare the vertical ZnO NWs. (b) the TEM cross-section image of AAO full of ZnO.

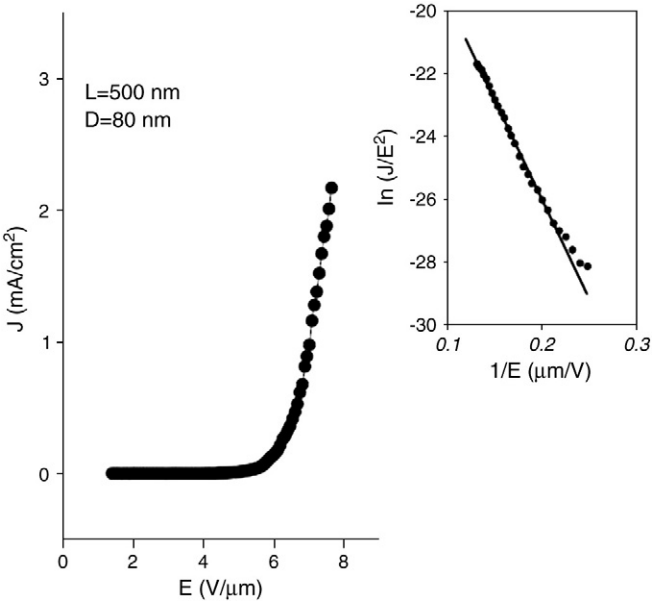

Fig. 3. Field-emission current density versus electric field for ZnO–NW with typical size of $L=500$ nm and $D=80$ nm. The inset shows the corresponding Fowler–Nordheim plots.

(AV^{-2} eV) and $B = 6.83 \times 10^3$ ($V\,eV^{-3/2}\,\mu m^{-1}$) [13]. Thus, the value of β can be calculated from the slope of the *F–N* plot, in which β is found to be about 1600 in this case. The field-emission ability and β value strongly depend upon the morphology of the ZnO NWs, including the geometry, structure tip size, and number of emitters on the substrate. Here we propose a simple way to examine roughly the E_{to}–β interdependence just from the *F–N* plot. The E_{to} value turns out approximately to be the reciprocal of the right end horizontal coordinate of the straight line in *F–N* plot. It means the slope has same inclination with E_{to}. With the slope relating to $1/\beta$, a small E_{to} corresponds to the higher β value. This may be attained intuitively by sharping the tip size, i.e., reducing the turn-on field via increasing the aspect ratio is expected to have a stronger field enhancement. This indicates one can get optimal E_{to} and β by L/D maximized. By glancing at the two straight lines in the inset of Fig. 4, one will expect the less steep one being with lower E_{to} and enhanced β.

3.3. Size effect

We verify this speculation by shrinking diameter down to 30 nm with $L/D = 500$ nm/80 nm for comparison. The corresponding *J–E* curve and *F–N* plot are shown in Fig. 4 for lines of white circle symbols. As expected, E_{to} is down to 2 V/μm and β up to 4000. The second line by black triangle symbol is for largest L of 1600 nm and smaller D of 30 nm to go forward in the case of maximized L/D. A profound enhancement of FE properties is obtained for $L/D = 53$ with E_{to} of 1.48 V/μm and β up to 6100. Separate length dependence is investigated on emitters length in the range of 500–1600 nm and keep $D = 80$ nm unchanged. Fig. 5 presents the results of measured E_{to} and calculated β. The consistency of reduced E_{to} and larger β is experimentally observed and confirmed by sharper tip size. One can probe this tendency with length via *J–E* in semi-log scale, as in Fig. 6. Data in Fig. 6 are chosen from Fig. 5 with $L = 500$, 1000, 1600 nm. The three segments in each curve represent different operation mode, so called respectively the off, active, saturation region with increasing field [22,23]. The middle active operation width implies the linear region in *F–N* plot. The fact that active E region width decreases with NW length agrees with the finding of a smaller *F–N* plot slope with a larger $1/E$ right end.

So far, the observed size-dependent variations of E_{to} and β are in expectation. However, several factors may have impacts on the

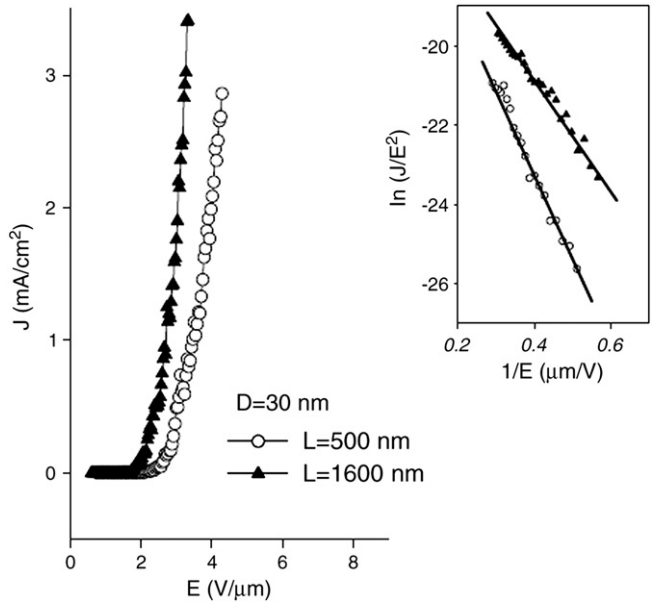

Fig. 4. The emission current density and the corresponding *F–N* plots in inset, with size *L–D* as labeled.

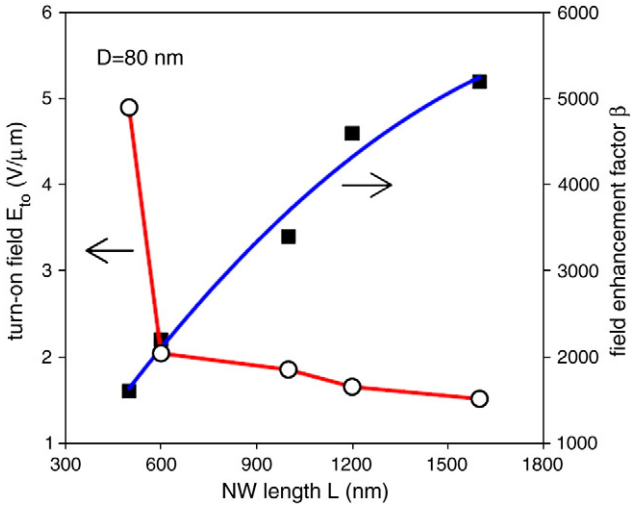

Fig. 5. Dependence of the turn-on field E_{to} and enhancement factor β on NW length L, with fixed diameter $D = 80$ nm.

feasibility of pursuing extreme L/D limit while keeping the effective improvement on FE effect. One is the process of hydrothermally grown ZnO within the nanochannels of the AAO templates. This poses the lower limit on D by considering the actual filling efficiency and self-assembly quality. The limitation on D is also physically determined by AAO interpore distance, which is controlled by the applied anodic voltage. Besides, the applied widening treatment to expand pore diameter simultaneously has the length shortening effect. The maximum length L available exists inevitably if simply extending the AAO growth time for formation of longer NWs. The phenomenon of uneven and large diameter of ZnO NW array should be considered, especially for those derived by chemical solution reaction compared with by vapor-phase approaches. It also needs dedicated techniques to synthesize high quality NWs at reasonable growth rate under low-temperature process. After all, large-scale, homogeneous, and dense NW arrays are essential for FE applications.

4. Conclusions

Field-emission measurement was conducted on nanowires based on ZnO 1-D nanostructure with high aspect ratio L/D. The size-dependent FE properties of lower E_{to} and higher β are verified in this study. We have prepared ZnO NWs based on two techniques. One is with the use of hydrothermal synthesis method to lower the fabrication temperature to 95 °C, and the other is with the aid of

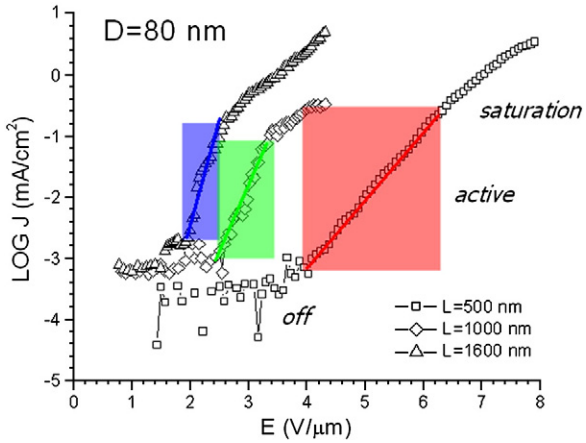

Fig. 6. Typical *J–E* curve in semi-log scale to highlight the active mode (middle segment by shadow) for FE. This operation region width decreases with NW length.

AAO template to facilitate the manipulation of NW's length and diameter growth.

References

[1] H. Rensmo, K. Keis, H. Lindstroem, S. Soedergren, A. Solbrand, A. Hagfeldt, S.E. Lindquist, L.N. Wang, M. Muhammed, J. Phys. Chem. B 101 (1997) 2598.
[2] Y. Lin, Z. Zhang, Z. Tang, F. Yuan, J. Li, Adv. Mater. Opt. Electron. 9 (1999) 205.
[3] J.Y. Lee, Y.S. Choi, J.H. Kim, M.O. Park, S. Im, Thin Solid Films 403 (2002) 553.
[4] M.H. Huang, S. Mao, H. Feick, H.Q. Yan, Y.Y. Wu, H. Kind, E. Weber, R. Russo, P.D. Yang, Science 292 (2001) 1897.
[5] K.S. Weissenrieder, J. Mueller, Thin Solid Films 300 (1997) 30.
[6] C.Y. Lee, T.Y. Tseng, S.Y. Li, P. Lin, J. Appl. Phys. 99 (2006) 24303.
[7] R.C. Wang, C.P. Liu, J.L. Huang, S.J. Chen, Appl. Phys. Lett. 88 (2006) 023111.
[8] S. Bhattacharyya, A. Rastogi, S.V. Bhat, K.S.R.K. Rao, A.V. Subramanyam, D. Kanjilal, Solid State Commun. 105 (1998) 543.
[9] Z.W. Pan, Z.R. Dai, Z.L. Wang, Science 291 (2001) 1947.
[10] J.J. Wu, S.C. Liu, Adv. Mater. 14 (2002) 215.
[11] J.Y. Lao, J.Y. Huang, D.Z. Wang, Z.F. Ren, Nano Lett. 3 (2003) 235.
[12] X.Y. Kong, Z.L. Wang, Appl. Phys. Lett. 84 (2004) 975.
[13] S.Y. Li, C.Y. Lee, P. Lin, T.Y. Tseng, J. Vac. Sci. Technol. B 24 (2006) 147.
[14] S.H. Jo, J.Y. Lao, Z.F. Ren, R.A. Farrer, T. Baldacchini, J.T. Fourkas, Appl. Phys. Lett. 83 (2003) 4821.
[15] X.Y. Xue, L.M. Li, H.C. Yu, Y.J. Chen, Y.G. Wang, T.H. Wang, Appl. Phys. Lett. 89 (2006) 43118.
[16] S.Y. Li, C.Y. Lee, T.Y. Tseng, J. Cryst. Growth 247 (2003) 357.
[17] W.I. Park, D.H. Kim, S.W. Jung, G.C. Yi, Appl. Phys. Lett. 80 (2002) 4232.
[18] B.D. Yao, Y.F. Chan, N. Wang, Appl. Phys. Lett. 81 (2002) 757.
[19] C.Y. Lee, S.Y. Li, P. Lin, T.Y. Tseng, IEEE Trans. Nanotechnol. 5 (2006) 216.
[20] S.H. Jeong, H.Y. Hwang, Kun-Hong Lee, Y. Jeong, Appl. Phys. Lett. 78 (2001) 2052.
[21] A.P. Li, F. Muller, A. Birner, K. Nielsch, U. Gosele, J. Appl. Phys. 84 (1998) 6023.
[22] J.M. Bonard, C. Klinke, Phys. Rev. B 67 (2003) 115406.
[23] C.Y. Lee, T.Y. Tseng, S.Y. Li, P. Lin, Nanotechnology 17 (2006) 83.